Ground Penetrating Radar Theory and Applications

I. L. Al-Qadi
S. Lahouar

ILLINOIS

Presentation Overview

- Background
  - Nondestructive Testing
  - GPR Systems
  - Electromagnetic Theory
  - GPR Data Analysis
- GPR Applications
  - Flexible Pavements
  - Rigid Pavements
  - Rail Road

ILLINOIS

Introduction

- US transportation infrastructure is deteriorating:
  - 2005 ASCE Report card for American Transportation Infrastructure gave an overall grade of "D" – estimated $1.3 trillion investment needed for improvements
- Transportation agencies are shifting efforts from building new to assessing and rehabilitating existing structures

ILLINOIS

What is NDE?

<u>N</u>on-<u>d</u>estructive <u>e</u>valuation

Detect defects, internal distresses, measure dimensions, etc. w/o damaging the material

- **Ultrasonic waves**
- **X-ray/ CAT scans**
- **RADAR scanning**
- **Thermal imaging**
- **etc**

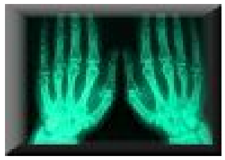

X-ray radiograph

ILLINOIS

What Are Waves?

Propagation of a *<u>disturbance</u>* through a medium (mass *<u>is not</u>* transported in propagation direction)

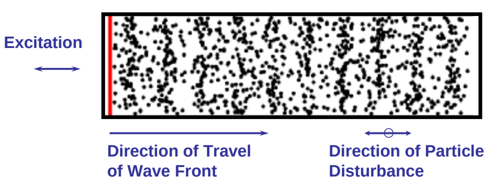

Important parameters:

wavelength (λ), period (T) and frequency (f)

ILLINOIS

Ultrasonic Testing (UT)

Flaw detection: wave echoes from air-filled defects such as cracks and voids

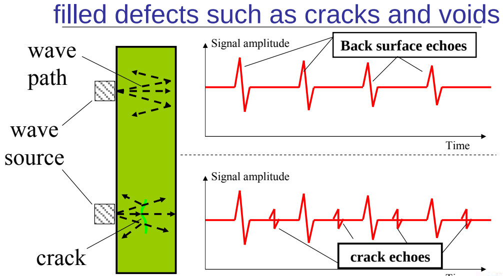

ILLINOIS

Ultrasonic Pulse Velocity (UPV)

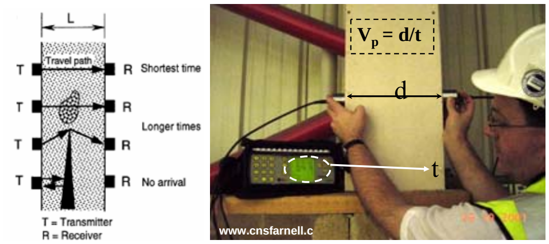

V_p related to in-place material strength or presence of internal voiding and cracking (Frequency 20-200MHz)

Approach Illustration

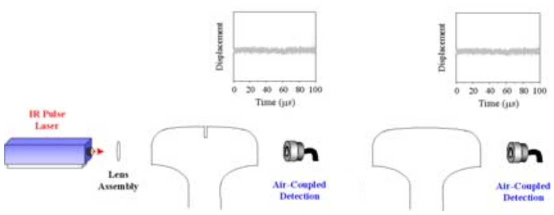

Crack **No Crack**

Impact Echo Principle (ASTM C1383)

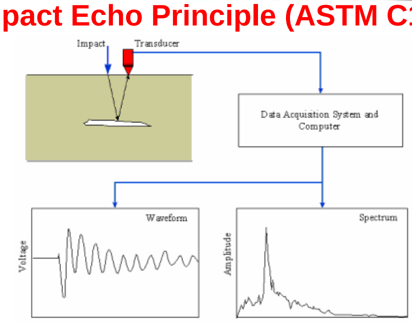

Reflected waves set up a resonance condition having a characteristic frequency (like a bell)

Concrete Element Inspection

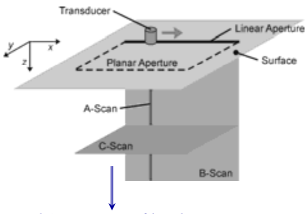

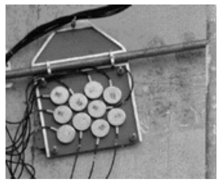

2- and 3-D maps of backscatter intensity (courtesy of BAM)

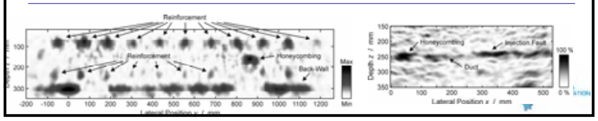

GPR Applications

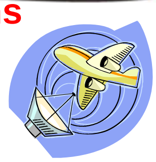

- Ground Penetrating Radar (GPR): special kind of RADAR
- GPR usage:
  1. Detect buried targets
  2. Estimate their depths
- GPR applications:
  - Geophysics: estimate structure of earth sediments
  - Archeology: locate buried archeological structures
  - Safety tool: locate landmines
  - Civil Engineering: evaluate performance of civil structures (buildings, bridges, pavements…)

GPR History

- Early 1900's: RADAR Principle Was Used to Detect Airborne Objects
- Hulsenberg (1926): Detection of Buried Objects
- Austria (1929): Depth of Glacier
- Late 1950's: US Air force plane crashed in Greenland because of wrong altitude from Radar

⇒ Ability of Radar to See Into Subsurface

GPR History

- 1960's: Moon Surface Characterization by NASA
  - Ground Probing Radar Systems Were Used in Geological Applications
- Vietnam War: "Combat Radar" Was Used to Locate Mines, Tunnels, and Bunkers
- 1970's: Locating Sewer Lines and Cables, Measuring Ice Thickness, Profiling Bottom of Lakes and Rivers
- 1980's-now: Different Applications Related to Pavements and Bridge Decks

ILLINOIS

EM Properties of Materials

Interaction of a Material with Applied Electric (E) and Magnetic (H) Fields:

- Polarization
- Conductivity
- Magnetic Permeability
- Permittivity/ Dielectric Constant

$$\varepsilon_r = \varepsilon_r^{'} - j\varepsilon_r^{''}$$

ILLINOIS

Polarization

- Electronic Polarization:
- Ionic Polarization:
- Molecular Polarization:
- Interfacial Polarization:

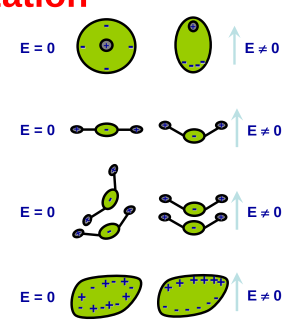

ILLINOIS

DIELECTRIC PROPERTIES OF CONCRETE

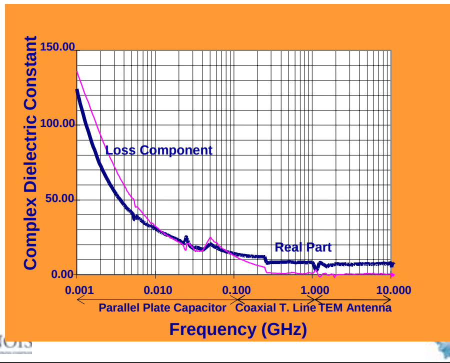

ILLINOIS

Typical Dielectric Constant Values

Material	Dielectric Constant
Air	1
Water	81
Concrete	3-18
HMA	3-10
Limestone	5-9
Granite	4-6
Dry Sand	3-5
Saturated Sand	20-30
Silts	5-30
Clays	5-40

ILLINOIS

GPR Types

Three main types of GPR systems:

- Frequency modulated GPR
- Synthetic pulse GPR
- Pulsed (or impulse) GPR

ILLINOIS

Frequency Modulated GPR

- Change frequency of transmitted signal linearly between two limits
- Frequency difference (transmitted - reflected) proportional to the layer depth

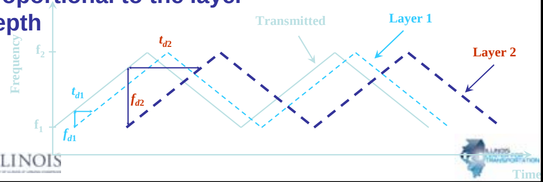

ILLINOIS

Synthetic Pulse GPR

- Change frequency of transmitted signal between two limits in discrete steps
- Amplitude and phase of reflected signal at each frequency step are recorded
- Reflected signal reconstructed in the time domain using an IFFT algorithm

ILLINOIS

Pulsed or Impulse GPR

- Most common type of GPR systems
- Transmitted signal is a short pulse (1 ns or less)
- Principle: Transmit a short pulse and record the reflected pulses from layer interfaces

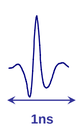

ILLINOIS

GPR Antennas

- Ground-coupled: the antenna is in contact with the ground surface
- Air-coupled: the antenna is 0.5m above surface
- Monostatic: one antenna used as Tx and Rx
- Bistatic: one antenna is used for Tx and another one for Rx

GPR: How does it work?

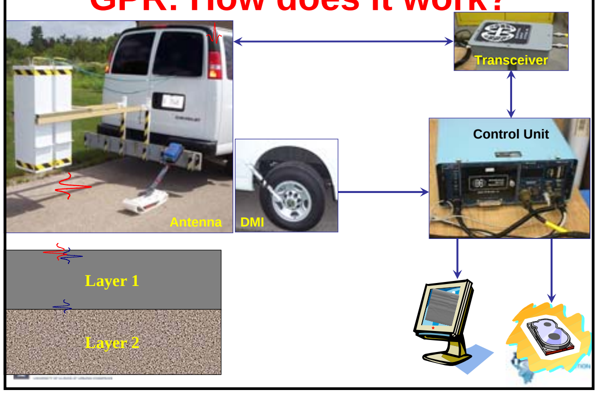

Reflection & Transmission

At normal incidence:

- Reflection coefficient: $\gamma = \frac{\eta_2 - \eta_1}{\eta_2 + \eta_1} = \frac{\sqrt{\varepsilon_{r1}} - \sqrt{\varepsilon_{r2}}}{\sqrt{\varepsilon_{r1}} + \sqrt{\varepsilon_{r2}}}$
- Transmission coefficient $\tau = \frac{2\eta_2}{\eta_1 + \eta_2} = \frac{2\sqrt{\varepsilon_{r1}}}{\sqrt{\varepsilon_{r1}} + \sqrt{\varepsilon_{r2}}}$

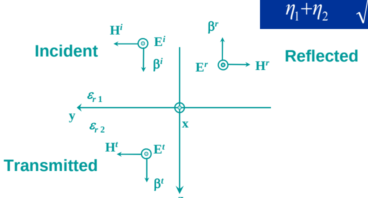

EM Scattering

- EM scattering: occurs when there is a *discontinuity* in the dielectric properties of a medium
- For pavements a discontinuity can be:
  - Layer interface
  - Distress within the layer
- At a discontinuity:
  - Reflection
  - Transmission

ILLINOIS

Typical GPR Response (scan)

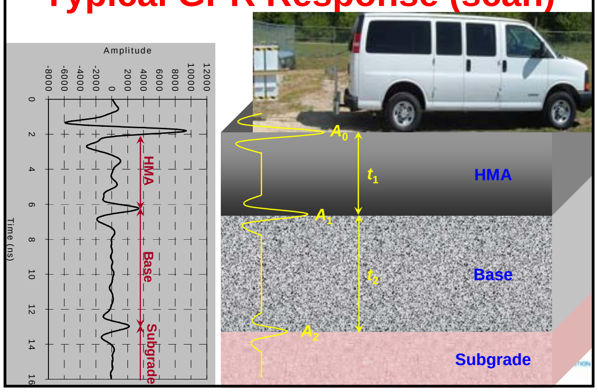

Typical Raw GPR Data

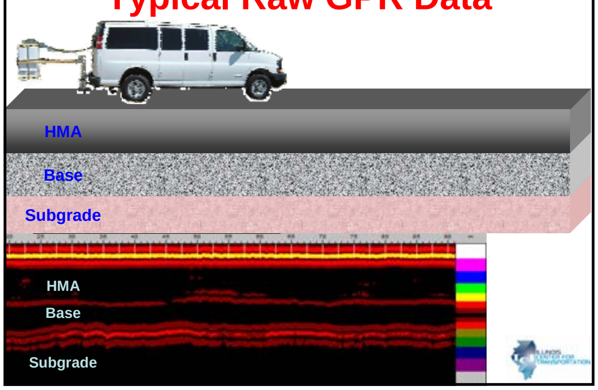

GPR Applications

- Layer thickness estimation
  - QC/QA: new pavements
  - Structure evaluation: in service pavements
- Subsurface Moisture/ Distress detection
- Rebar/ Dowel Localization
- Rebar Cover Depth Estimation
- Railroad Evaluation (Ballast)

ILLINOIS

Typical Problems with GPR Data Interpretation

- GPR doesn't provide "real" images of the subsurface
- Dielectric properties unknown
  - Dielectric properties change with depth (especially in the presence of moisture)
- Thin pavement layers are difficult to resolve
- Extensive amount of data
- GPR results are operator dependent

ILLINOIS

Layer Thickness Estimation

Thickness of i th layer:

$$d_i = \frac{ct_i}{2\sqrt{\varepsilon_{r,i}}}$$

where: $\varepsilon_{r,1} = \left(\frac{A_p - A_o}{A_p + A_o}\right)^2$,

$$\varepsilon_{r,n} = \varepsilon_{r,n\text{-}1}\left(\frac{1-\left(\frac{A_0}{A_p}\right)^2+\sum_{i=1}^{n-2}\gamma_i\frac{A_i}{A_p}+\frac{A_{n-1}}{A_p}}{1-\left(\frac{A_0}{A_p}\right)^2+\sum_{i=1}^{n-2}\gamma_i\frac{A_i}{A_p}-\frac{A_{n-1}}{A_p}}\right)^2$$

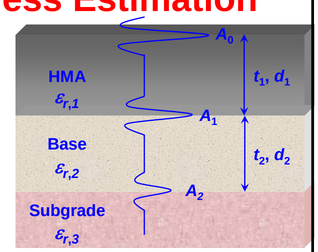

$$\gamma_i = \frac{\sqrt{\varepsilon_{r,i}} - \sqrt{\varepsilon_{r,i+1}}}{\sqrt{\varepsilon_{r,i}} + \sqrt{\varepsilon_{r,i+1}}}$$

ILLINOIS

GPR: EMBEDDED COPPER PLATES

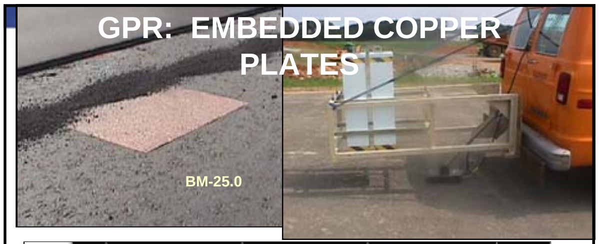

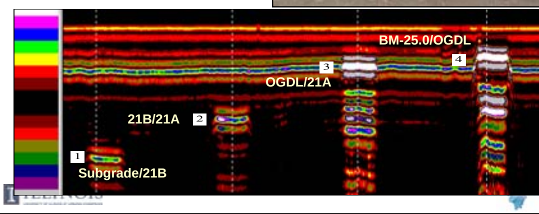

WS Dielectric Constant

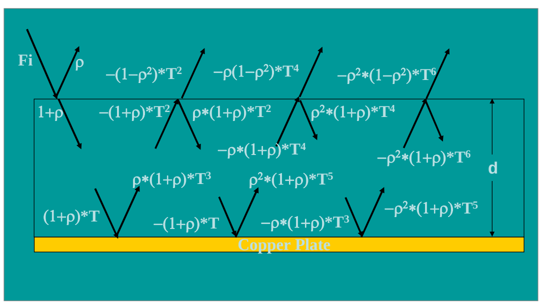

Multiple Reflection Model

Input Reflection Coefficient

$$\Gamma = \frac{FT(Y_r)}{FT(Y_i)} = \frac{F_r}{F_i} = \rho - T^2\,(1-\rho^2)\frac{1-(\rho T^2)^{n+1}}{1-\rho T^2} = \rho - T^2\,(1-\rho^2)\sum_{i=1}^{n}(\rho T^2)^i$$

with: $\rho = \dfrac{1-\sqrt{\varepsilon_r^*}}{1+\sqrt{\varepsilon_r^*}}$ and $T = e^{-j\frac{\omega}{c}\sqrt{\varepsilon_r^*}\,d} = e^{-j\frac{\omega}{c}\frac{1-\rho}{1+\rho}d}$

To find ε_r, Solve: $f(\rho) = \rho - T^2\,(1-\rho^2)\dfrac{1-(\rho T^2)^{n+1}}{1-\rho T^2} - \dfrac{F_r}{F_i} = 0$

Multiple Solutions

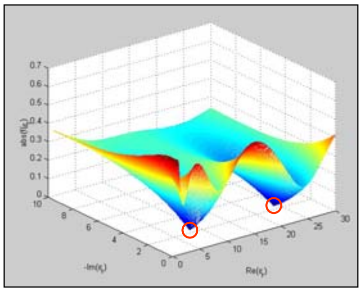

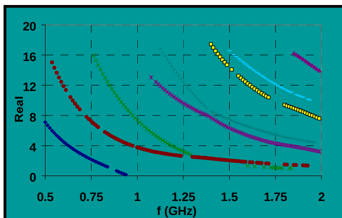

Real Solutions

Imaginary Solutions

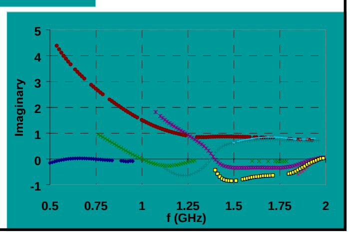

Physical Solution

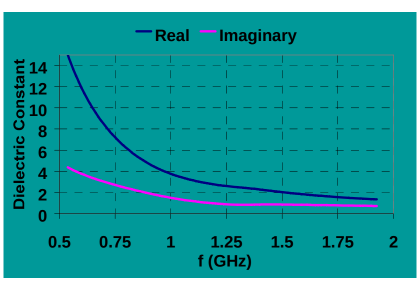

Dielectric Constant for SM-12.5D

Thickness Estimation Using CMP Technique (more accurate)

Common midpoint (CMP) technique (or common-depth point, CDP) is used as follows:

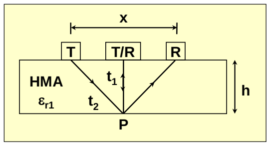

$$vt_2 = 2\sqrt{h^2 + \left(\frac{x}{2}\right)^2}$$

$$v = \frac{c}{\sqrt{\varepsilon_r}} = \frac{x}{\sqrt{t_2^2 - t_1^2}}$$

v: EM velocity in the layer

$$vt_1 = 2h \quad \Rightarrow \quad \varepsilon_r = \frac{c^2\left(t_2^2 - t_1^2\right)}{x^2}$$

ILLINOIS

Thickness Estimation Using Modified CMP Technique

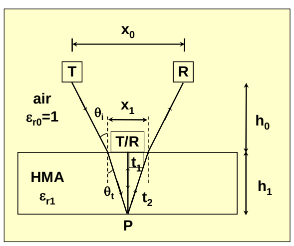

Snell's law of refraction:

$$\sqrt{\varepsilon_{r0}}\sin\theta_i = \sqrt{\varepsilon_{r1}}\sin\theta_t \quad \textbf{(1)}$$

Using the figure:

$$2h_0 \tan\theta_i + x_1 = x_0 \quad \textbf{(2)}$$

$$\tan\theta_t = \frac{x_1}{2h_1} = \frac{x_1}{vt_1} \quad \textbf{(3)}$$

$$v = \frac{x_1}{\sqrt{t_2^2 - t_1^2}} \quad \textbf{(4)}$$

ILLINOIS

Thickness Estimation Using Modified CMP Technique

Algorithm:

1. **Measure the reflection times t_1 and t_2**
2. **Calculate the transmission angle θ_t using:** $\tan\theta_t = \frac{\sqrt{t_2^2 - t_1^2}}{t_1}$
3. **Find the angle θ_i by solving numerically**

$$2h_0 \tan\theta_i + c\frac{\sin\theta_t}{\sin\theta_i}\sqrt{t_2^2 - t_1^2} = x_0$$

4. **Solve for ε_{r1} using:** $\varepsilon_{r1} = \left(\frac{\sin\theta_i}{\sin\theta_t}\right)^2$
5. **Compute HMA thickness using t_1 and ε_{r1}** $\quad h_1 = ct_1 / 2\sqrt{\varepsilon_{r1}}$


Modified CMP Setup

ILLINOIS

Automated GPR Data Analysis

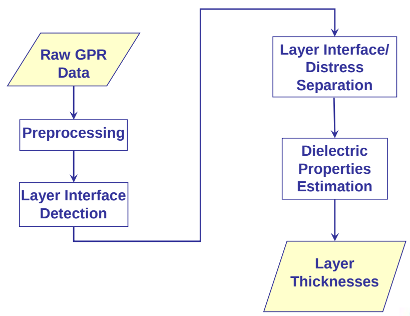

ILLINOIS

Preprocessing

Enhance signal quality:
- Noise filtering
- Coupling pulse removal

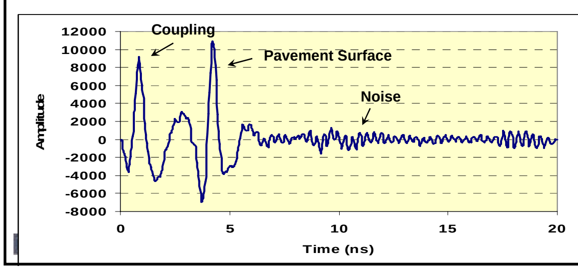

Noise Filtering

- GPR susceptible to EM noise: CB radios, cell phones, cell phone towers, etc.

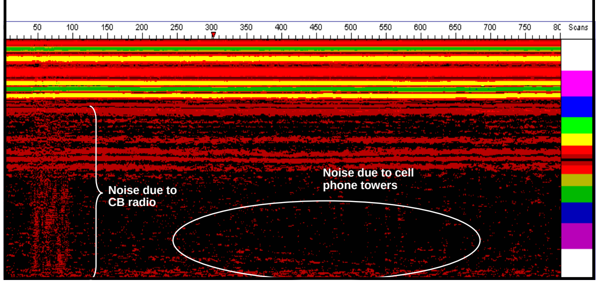

Noise Filtering

Elliptic low-pass filter: most efficient filter

- Lowest order ➔ fast to run on data
- Lowest transition bandwidth ➔ high performance

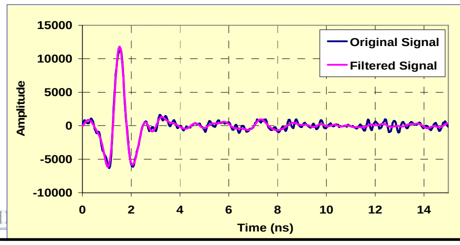

Coupling Pulse Removal: Makes Analysis Easier!

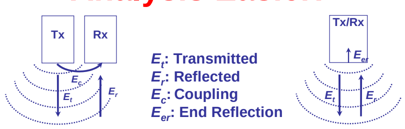

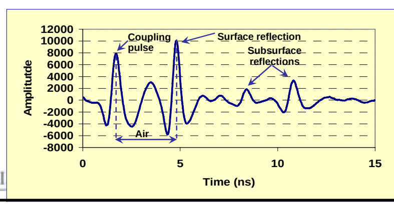

Coupling Pulse Removal Procedure

Coupling pulse, $y_c(t)$, measurement

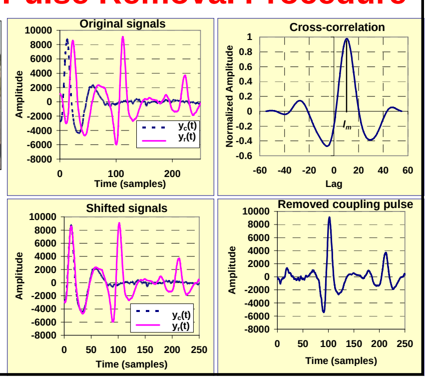

Preprocessing Results

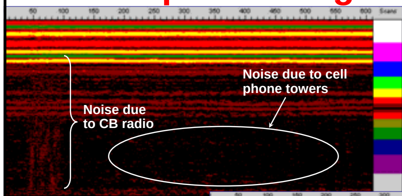

Raw GPR Data

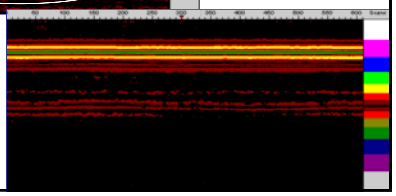

After Filtering & Coupling Removal

ILLINOIS

GPR Depth Resolution

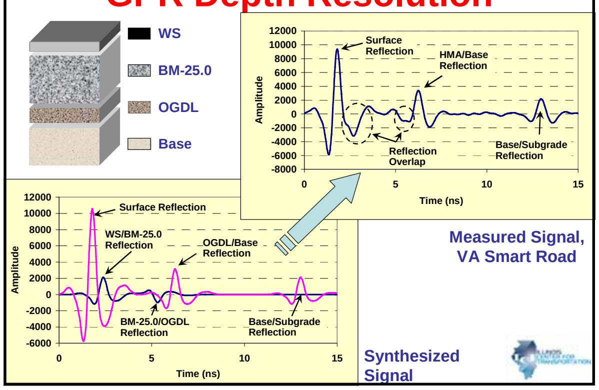

Measured Signal, VA Smart Road

Synthesized Signal

GPR Depth Resolution

Depth resolution: $\Delta d = \dfrac{cT}{2\sqrt{\varepsilon_r}}$

- *T*: Pulse width
- ε_r: Dielectric Constant

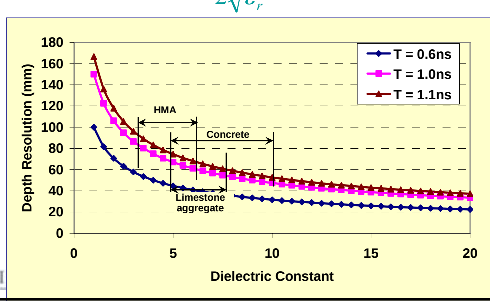

GPR Detection Limitations

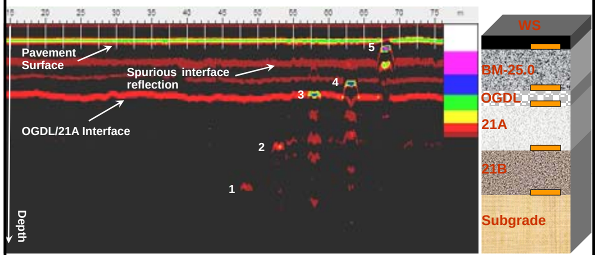

Copper Plate Reflections at the (1) 21B/Subgrade, (2) 21A/21B, (3) OGDL/21A, (4) BM-25.0/OGDL, and (5) WS/BM-25.0 Interfaces; Section A

ILLINOIS

Depth Resolution Enhancement

- Inverse filtering
- Predictive deconvolution
- Pulse spiking
- Pulse shaping
- Homomorphic deconvolution

(Inverse filtering, predictive deconvolution, pulse spiking and pulse shaping: Wiener Filter)

ILLINOIS

Inverse Filtering

- Implemented as a Wiener filter
- Desired output: impulse at time t=0 ⇒ δ(t)
- Incident signal assumed unknown
- Filter designed according to:

$$\begin{bmatrix} r_{yy}(0) & r_{yy}(1) & r_{yy}(2) & \cdots & r_{yy}(N-1) \\ r_{yy}(1) & r_{yy}(0) & r_{yy}(1) & \cdots & r_{yy}(N-2) \\ r_{yy}(2) & & r_{yy}(0) & & r_{yy}(N-3) \\ \vdots & & & \ddots & \vdots \\ r_{yy}(N-1) & \cdots & \cdots & \cdots & r_{yy}(0) \end{bmatrix} \begin{bmatrix} a_0 \\ a_1 \\ a_2 \\ \vdots \\ a_{N-1} \end{bmatrix} = \begin{bmatrix} 1 \\ 0 \\ 0 \\ \vdots \\ 0 \end{bmatrix}$$

ILLINOIS

Predictive Deconvolution

- Implemented as a Wiener filter
- Desired output: reflected signal advanced by α samples ⇒ *y*(*t*+ *α*)
- Incident signal assumed unknown
- Filter designed according to:

$$\begin{bmatrix} r_{yy}(0) & r_{yy}(1) & r_{yy}(2) & \cdots & r_{yy}(N-1) \\ r_{yy}(1) & r_{yy}(0) & r_{yy}(1) & \cdots & r_{yy}(N-2) \\ r_{yy}(2) & & r_{yy}(0) & & r_{yy}(N-3) \\ \vdots & & & \ddots & \vdots \\ r_{yy}(N-1) & \cdots & \cdots & \cdots & r_{yy}(0) \end{bmatrix} \begin{bmatrix} a_0 \\ a_1 \\ a_2 \\ \vdots \\ a_{N-1} \end{bmatrix} = \begin{bmatrix} r_{yy}(\alpha) \\ r_{yy}(\alpha+1) \\ r_{yy}(\alpha+2) \\ \vdots \\ r_{yy}(\alpha+N-1) \end{bmatrix}$$

ILLINOIS

Pulse Spiking

- Implemented as a Wiener filter
- Desired output: an impulse (or spike) at a lag *l*
- Incident signal should be known
- Filter designed according to:

$$\begin{bmatrix} r_{xx}(0) & r_{xx}(1) & r_{xx}(2) & \cdots & r_{xx}(N-1) \\ r_{xx}(1) & r_{xx}(0) & r_{xx}(1) & \cdots & r_{xx}(N-2) \\ r_{xx}(2) & & r_{xx}(0) & & r_{xx}(N-3) \\ \vdots & & & \ddots & \vdots \\ r_{xx}(N-1) & \cdots & \cdots & \cdots & r_{xx}(0) \end{bmatrix} \begin{bmatrix} a_0 \\ a_1 \\ a_2 \\ \vdots \\ a_{N-1} \end{bmatrix} = \begin{bmatrix} x(l) \\ x(l-1) \\ \vdots \\ x(0) \\ 0 \\ \vdots \\ 0 \end{bmatrix}$$

ILLINOIS

Pulse Shaping

- Implemented as a Wiener filter
- Desired output: a pulse with a fixed shape *s*(*t*) at a given lag *l*
- Incident signal should be known
- Filter designed according to:

$$\begin{bmatrix} r_{xx}(0) & r_{xx}(1) & r_{xx}(2) & \cdots & r_{xx}(N-1) \\ r_{xx}(1) & r_{xx}(0) & r_{xx}(1) & \cdots & r_{xx}(N-2) \\ r_{xx}(2) & & r_{xx}(0) & & r_{xx}(N-3) \\ \vdots & & & \ddots & \vdots \\ r_{xx}(N-1) & \cdots & \cdots & \cdots & r_{xx}(0) \end{bmatrix} \begin{bmatrix} a_0 \\ a_1 \\ a_2 \\ \vdots \\ a_{N-1} \end{bmatrix} = \begin{bmatrix} r_{sx}(l) \\ r_{sx}(l+1) \\ r_{sx}(l+2) \\ \vdots \\ r_{sx}(l+N-1) \end{bmatrix}$$

ILLINOIS

Homomorphic Deconvolution

- **Power cepstrum of signal *y*(*t*):**

$$C_y(q) = \left| F\left\{ \log\left[\left| F\{y(t)\} \right|^2 \right] \right\} \right|^2$$

- **For GPR reflected signals:**

$$C_y(q) \approx \left| F\left\{ \log[\Phi_x(f)] + \log\left[A_0^2\right] + 2\sum_{n=1}^{N-1} \frac{A_n}{A_0} \cos(2\pi f \sum_{i=1}^{n} t_i) \right\} \right|^2$$

- **Term inside brackets periodic function of time delays ⇒ Power cepstrum composed of pulses corresponding to time-delays**

ILLINOIS

Typical Results

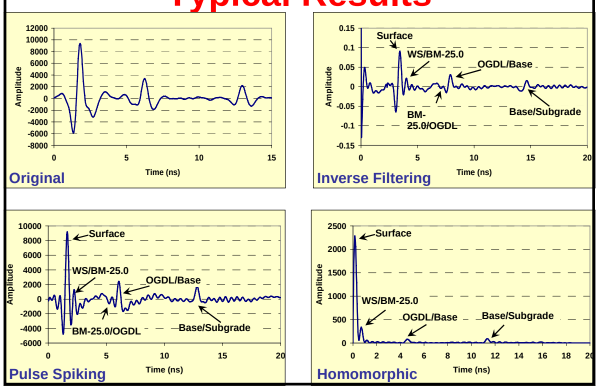

Typical Results: Inverse Filtering

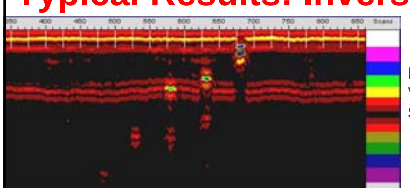

Raw Data, VA. Smart Road, Section A

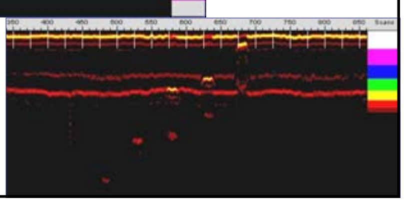

Processed Data

ILLINOIS

Resolving Thin Layers (Deconvolution)

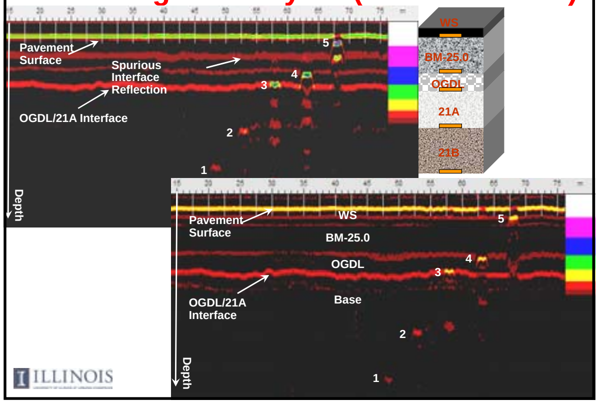

ILLINOIS

Layer Interface Detection

- Purpose:
- Detect layer interface reflections
- Estimate layer interface reflection time-delays

TD reflected signal:

$$y_r(t) = \sum_{i=0}^{N-1} A_i x(t - \sum_{j=0}^{i} t_j) + n(t)$$

$x(t)$: Incident signal
$n(t)$: Additive noise

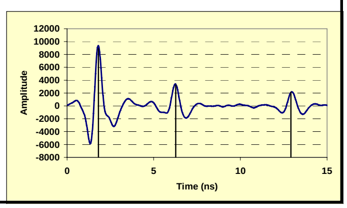

ILLINOIS

Detection of Multiple Layers

Combined detection/estimation

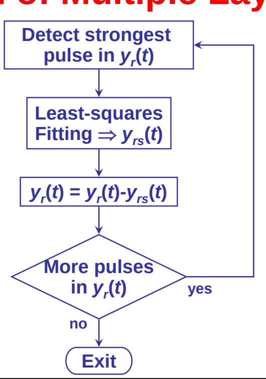

ILLINOIS

Detected Layer Interfaces

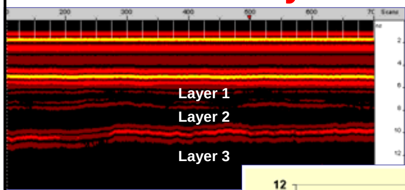

Raw GPR Data

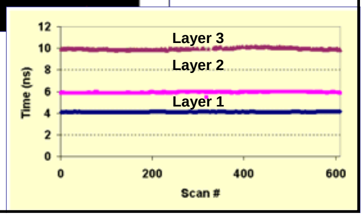

Detected Time Delays

Dielectric Constant/ Thickness

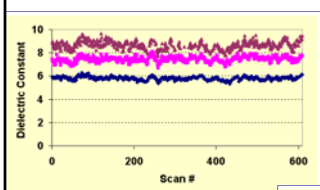

Dielectric Constant Results

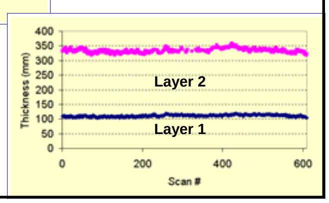

Layer Thickness Results

GPRan: GPR Data Analysis Software

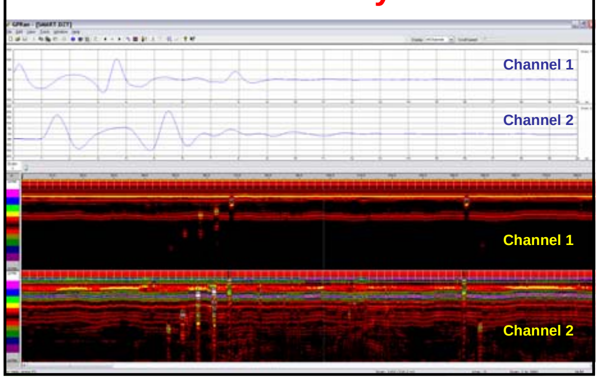

GPRan: Data Analysis Window

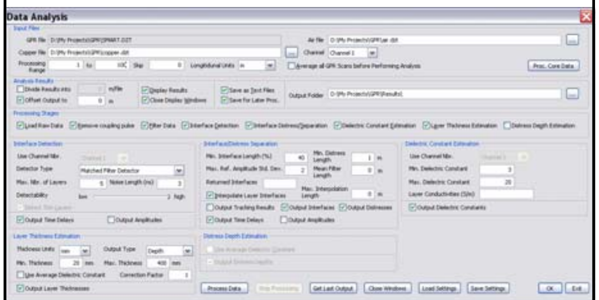

ILLINOIS

GPRan: Data Analysis Results

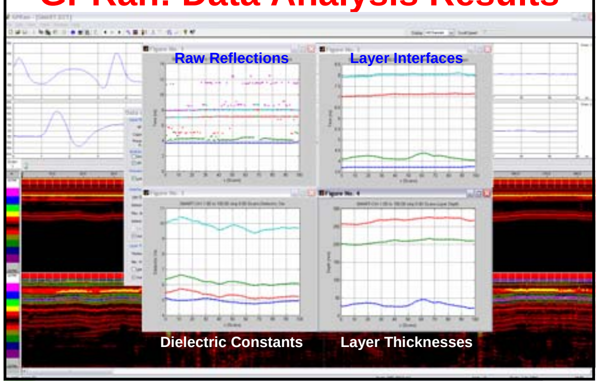

Case Studies: I-81

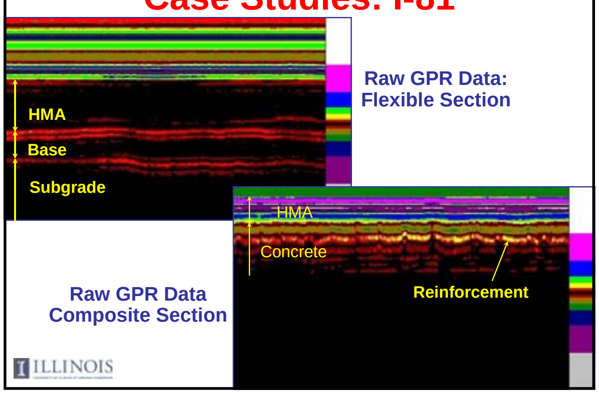

ILLINOIS

Case Studies: I-81

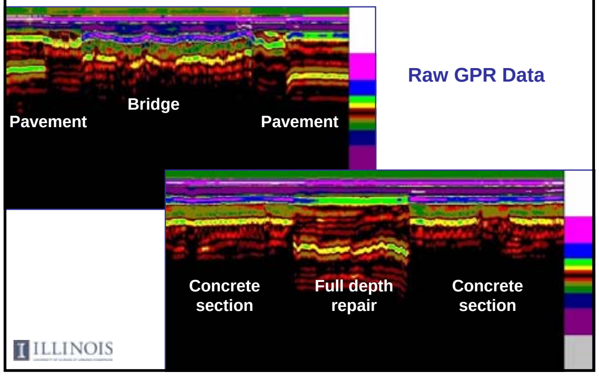

Raw GPR Data

ILLINOIS

HMA Thickness from GPR, I-81

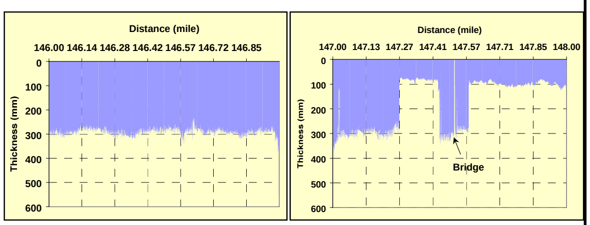

Flexible Section (1mile) Composite Section (1mile)

ILLINOIS

HMA Thickness Error, I-81

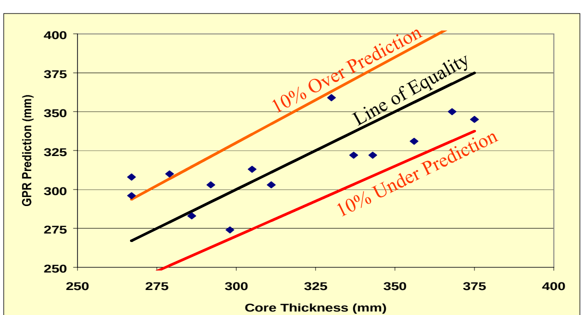

ILLINOIS

QA/QC New Pavement (VA Rt. 288)

Pavement design:

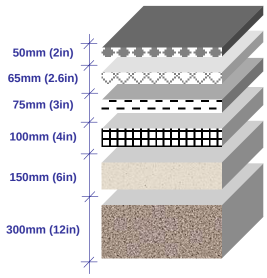

- SM-12.5 w/ PG 76-22
- IM-19.0 (2) w/ PG 76-22
- IM-19.0 (1) w/ PG 64-22
- BM-25.0 w/ PG 64-22
- 21-B aggregate base
- Lime stabilized subgrade

ILLINOIS

GPR Data Collection (Rt. 288)

- GPR surveys were performed on each layer after its construction
- Three surveys were performed per lane and per layer; in total, 36 surveys were performed
- DMI set at 10 scans/m
- For HMA layers, static measurements were taken near core locations

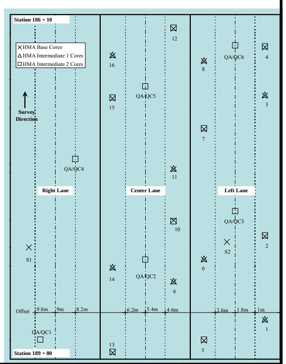

ILLINOIS

Typical GPR Response (Rt. 288)

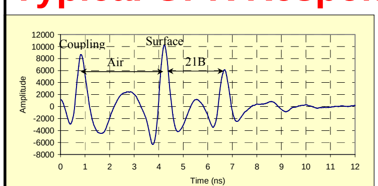

GPR Scan over 21-B Layer

GPR Scan over HMA Intermediate 2

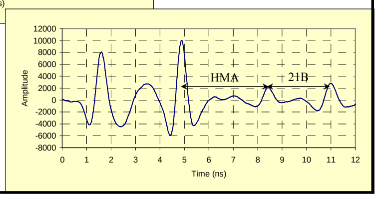

ILLINOIS

21-B Thickness (Rt 288)

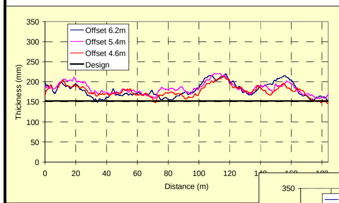

Center Lane, 0-184 m

Offset values are with respect to left edge of left lane

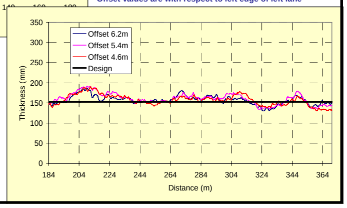

Center Lane, 184-370 m

ILLINOIS

HMA Intermediate-2 Thickness (Rt 288)

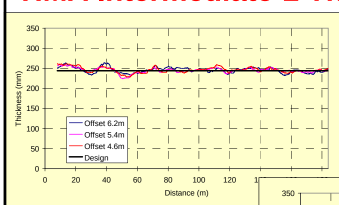

Center Lane, 0-184 m

Offset values are with respect to left edge of left lane

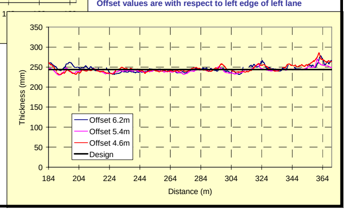

Center Lane, 184-370 m

ILLINOIS

Overall Thickness (Rt 288)

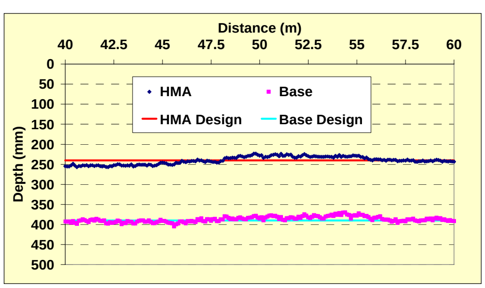

ILLINOIS

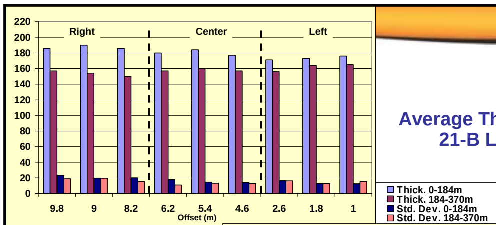

Average Thickness, 21-B Layer

Offset values are with respect to left edge of left lane

Average Thickness, HMA Base Layer

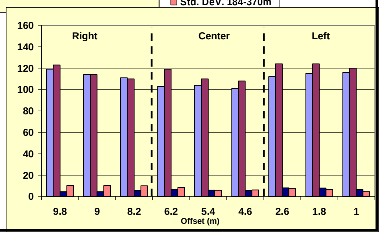

ILLINOIS

GPR Accuracy (Rt 288)

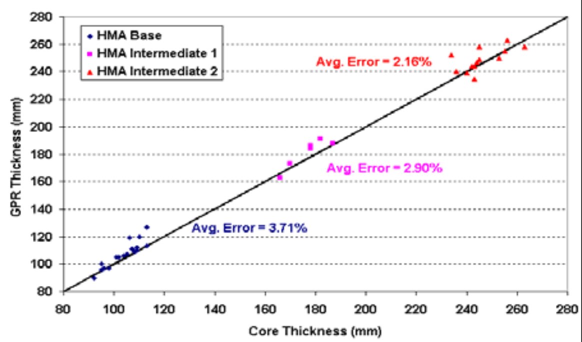

Case Study: 18 Premium Pavement Sites

- Sites located mainly on highways
- Different types of pavements were tested:
  - Full-depth flexible pavement
  - Rigid (jointed plain concrete pavement (JPCP)
  - Continuously reinforced concrete (CRCP)
  - Composite pavement
- Each section was 0.8 km (0.5 mile) long

ILLINOIS

Test Sites (Part)

Site #	County	Route	Direction	Milepost*	Pavement Type	Age (yrs)
1	Amherst	29	South	7.80-7.30	Flexible	15
2	Albemarle	64	East	12.99-13.37	Comp. CRC (rehab)	>20 (Surf.>10)
3	Louisa	64	West	9.91-9.41	Flexible	>20 (Surf.<10)
4	Louisa	64	West	2.28-1.78	CRC	15
7	York	64	West	22.23-24.71	JPCP	0-5
8	Suffolk	58	East	25.50-26.00	Comp. (new)	>20 (Surf.<10)
9	Washington	81	South	1.50-1.00	Flexible	0-5

ILLINOIS

Data Collection: 18 Prem. Sites

- GPR data were taken in the traveling lane at two transverse locations (center and right wheel path)
- GPR data acquisition frequency:
  - Flexible sections: 1scan/0.3m (1ft) using air-coupled antenna
  - JPCP and composite sections (without rebar): 1scan/0.3m (1ft) using air-coupled and ground-coupled antennae.
  - Composite sections (with rebar): 1scan/25mm (1in) using air-coupled and ground-coupled antennae

ILLINOIS

Raw GPR Data: 18 Prem. Sites

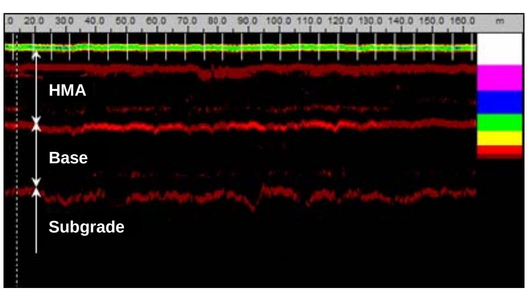

ILLINOIS

GPR Results: 18 Prem. Sites (Flexible)

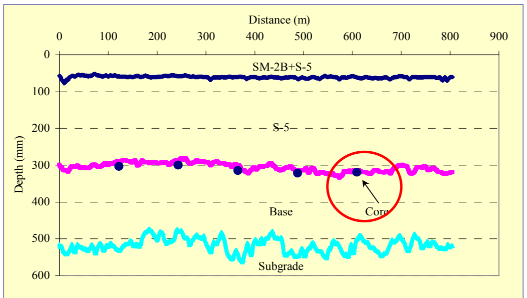

ILLINOIS

GPR Results: 18 Prem. Sites (Rigid)

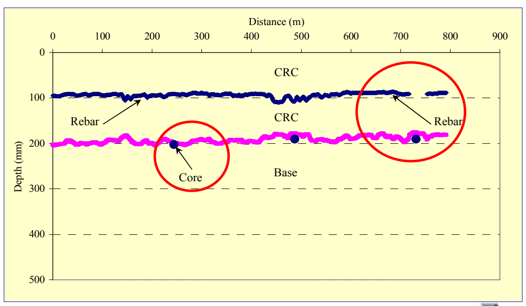

ILLINOIS

GPR Accuracy (18 Prem. Sites)

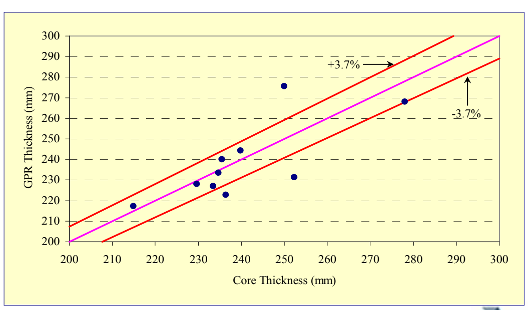

ILLINOIS

Average Error per Site (18 Prem. Sites)

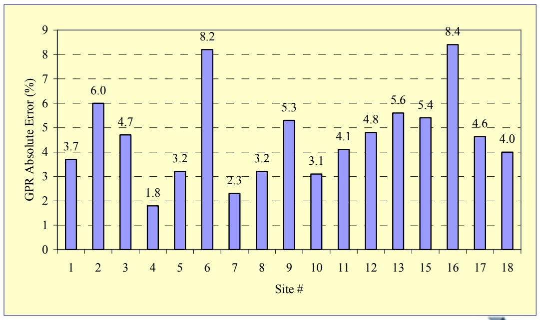

Average Error per Age (18 Prem. Sites)

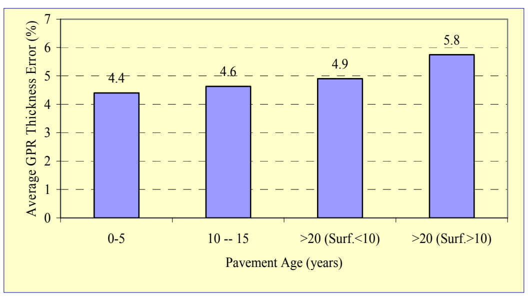

Average Error per Type (18 Prem. Sites)

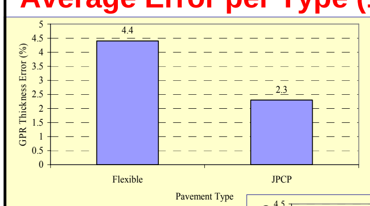

Pavement Age: 0-5 yrs

Pavement Age: 10-15 yrs

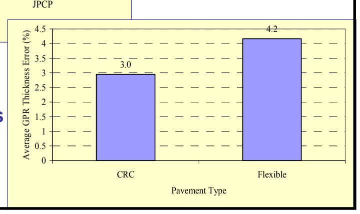

Locating Subsurface Moisture

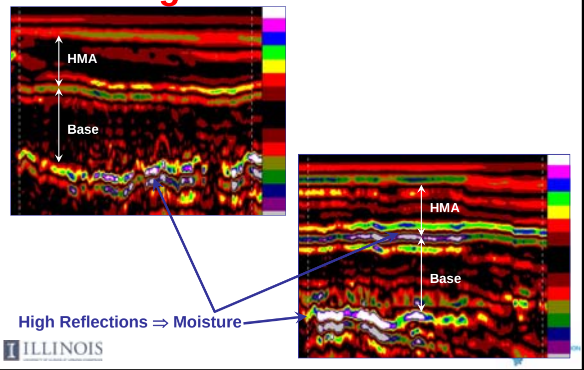

Geocomposite: Moisture Barrier?

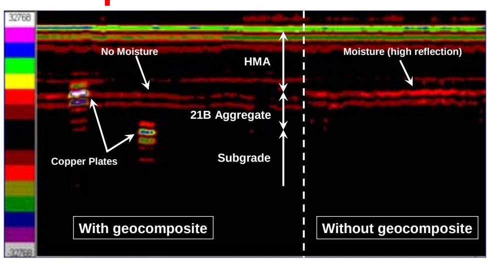

Ground-Coupled GPR Data, VA. Smart Road, Section J

Locating Reinforcing Mesh

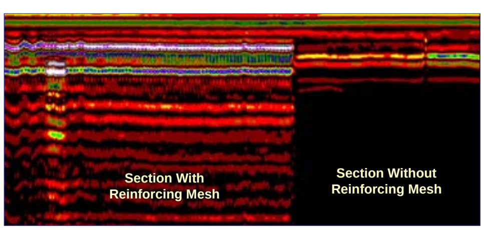

Ground-Coupled Data, VA. Smart Road, Section L

QC of Mesh Installation

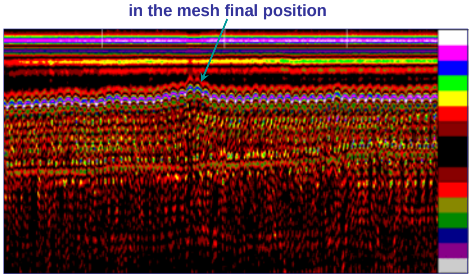

Ground-Coupled Data, VA. Smart Road, Section I

Locating Reinforcement Using GPR

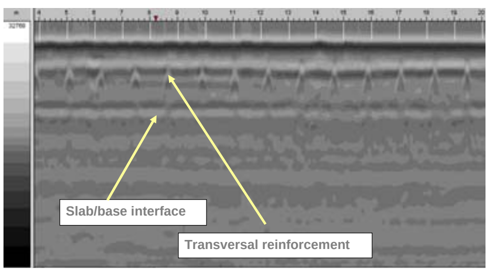

Locating Reinforcement (CRCP)

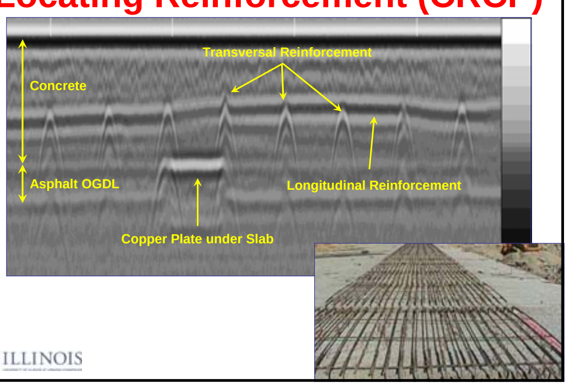

Raw GPR Data

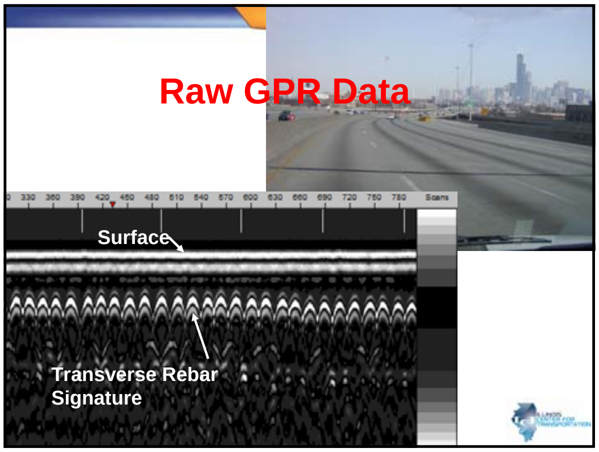

Locating Dowels (JPCP)

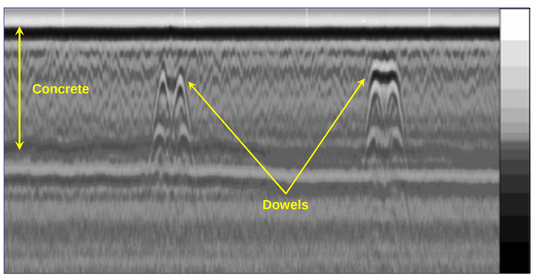

Ground-Coupled Data, JPCP, VA. Smart Road

ILLINOIS

Rebar Cover-Depth Estimation

GPR antennas receive EM signals reflected by rebar at different locations

⇒ Parabolic Shape

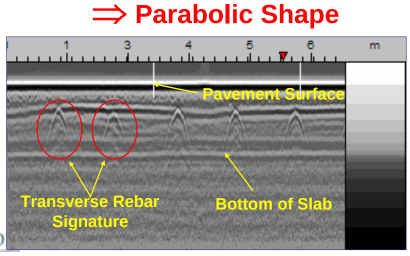

ILLINOIS

GPR Data Collection

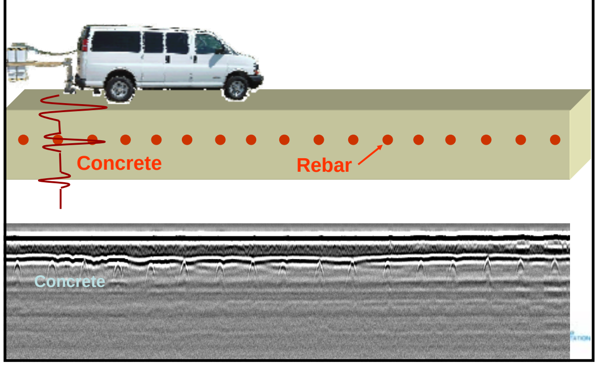

Rebar Cover-Depth Estimation

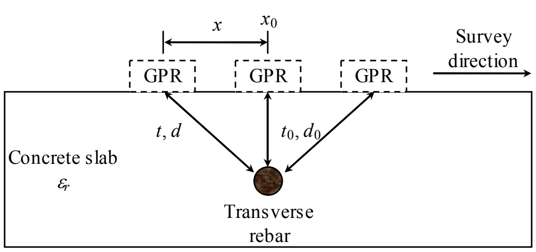

Survey configuration on CRCP

ILLINOIS

Rebar Cover-Depth Estimation

From the previous configuration we have:

$$t^2 = \frac{4}{v^2}x^2 - \frac{8x_0}{v^2}x + t_0^2 + \frac{4x_0^2}{v^2}$$

with: $v = \frac{c}{\sqrt{\varepsilon_r}}$

ILLINOIS

Rebar Cover-Depth Estimation Algorithm

- Measure the time *t* and the distance *x* from GPR data (using image processing techniques)
- Estimate the parameters v, t_0, and x_0 by nonlinearly fitting *t* and *x* to the model
- Estimate the dielectric constant ε_r
- Estimate the rebar cover-depth d_0:

$$d_0 = \frac{vt_0}{2}$$

ILLINOIS

Parabolic Shape Extraction from GPR Data

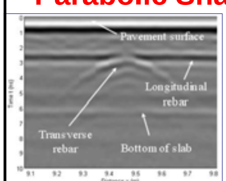

Removal of unwanted reflections

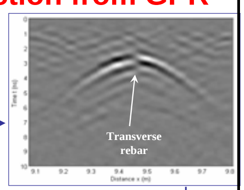

Image Thresholding

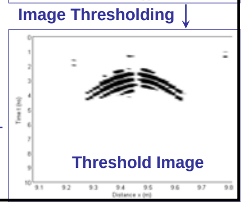

Detected *t* and *x*

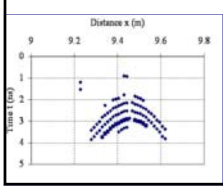

Rebar Cover-Depth Results

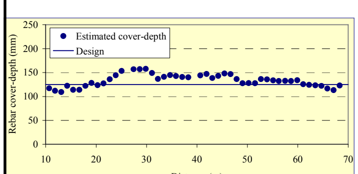

CRCP Section with cement OGDL

CRCP Section with asphalt OGDL

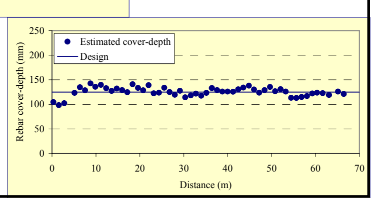

ILLINOIS

Rebar Cover-Depth Accuracy

Comparison of GPR estimated cover-depth to CRCP cores from the VA Smart Road

	Core cover-depth (mm)	*GPR cover-depth (mm)*	*Error (%)*
Core 1	145	141	2.8
Core 2	121	118	2.5
Average error (%)			2.6

ILLINOIS

Railroad Structure

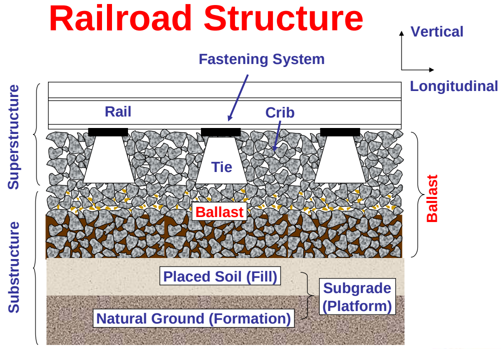

ILLINOIS

Clean and Fouled Ballast

Ballast fouling greatly influences its functions:

- **Clean ballast : made of uniformly graded aggregates ⇒ large air voids.**
- **Fouled ballast : fouled by fine-grained material that the fills air-voids.**

ILLINOIS

Dielectric Characteristics of Ballast

Dielectric constants of quartzite ballast

Railroad Ballast	Dielectric Constant
Dry, Clean Ballast	3.0
Wet, Clean Ballast (5% water)	3.5
Dry, Spent Ballast	4.3
Wet, Spent Ballast (5% water)	7.8
Saturated, Spent Ballast	38.5

– *Effect of moisture on fouled ballast is much greater than on clean ballast*

ILLINOIS

Scattering Analysis

- **Pavement Materials:**
  - Scattering response is small
  - Reflected pulse has similar shape as incident signal
- **Railroad Ballast:**
  - Scattering response is dominant (heterogeneousity is high)
  - Reflected pulse shape is influenced by scatter - air void

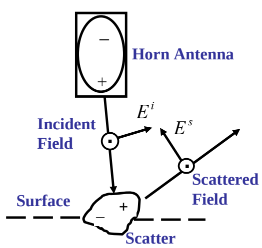

ILLINOIS

EM Scattering from Air-Voids (cont.)

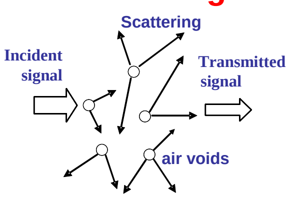

Attenuation Coefficient:

$$\alpha_s = \frac{N \cdot A}{2}$$

$$E = E_0 \cdot e^{-\alpha_s \cdot L}$$

N: number of particles per unit volume

Ballast degradation ⇒ Less air-voids ⇒ Less scattering ⇒ Less attenuation

ILLINOIS

GPR Data Collection on Railroad

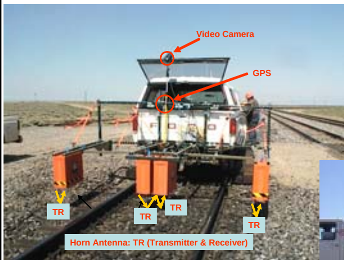

ILLINOIS

GPR Data Processing

Digital Signal Processing performed during data collection:

- Vertical band-pass FIR filter to remove noise
- Horizontal band-pass filter to remove clutter from rails
- Gain to account for energy attenuation

ILLINOIS

Processed GPR Data

First pulse from surface and subsequent small pulses are mainly from scattering

Raw GPR data

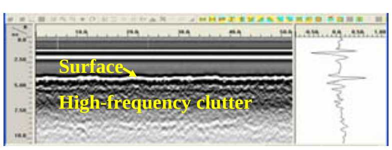

Processed GPR data

ILLINOIS

Trapped Water Detection

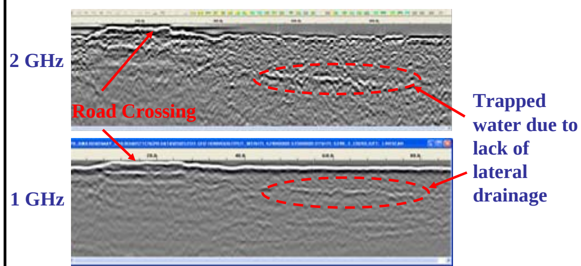

2 GHz antenna is more sensitive to scattering pattern change than 1 GHz antenna.

ILLINOIS

Scattering Analysis of Ballast under Different Conditions

GPR Data for different fouling conditions

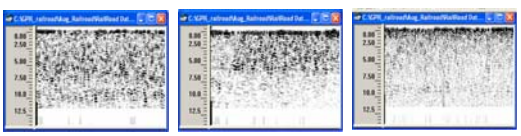

(a) Clean (b) Moderately fouled (c) Fouled

Ballast exhibiting various scattering patterns

Note: When ballast becomes fouled, interface between clean and fouled ballast is more difficult to find.

ILLINOIS

Ballast Breakdown

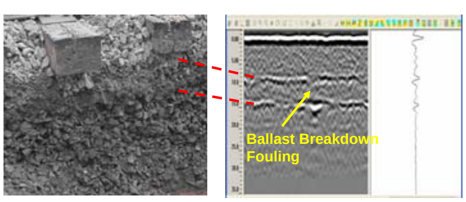

Ballast breakdown under sleepers.

ILLINOIS

Summary

- GPR is a NDE technique that can be used effectively to evaluate various transportation structures
- GPR can provide quick and reliable information about the subsurface.
- GPR reliable applications include:
  - Layer thickness estimation
  - Subsurface Moisture/ Distress detection
  - Rebar cover depth estimation
  - Rail Road evaluation (Ballast)
  - …

ILLINOIS

Thank You!

Questions?

ILLINOIS